Indian Journal of Chemistry
Vol. 60A, March 2021, pp. 361-369

Electron transfer study on newly synthesized Ti(IV)/Zr(IV) complexes of amide and oxime functionality: A pulse radiolytic and theoretical revelation

Raji Thomas[a,]*, Densely Jose[b], Nelson Joseph P[c], R T Pardasani[d] & T Mukherjee[e]

[a]Department of Chemistry, School of Science and Humanities, Sreenidhi Institute of Science & Technology, Hyderabad 501 301, India

[b]Department of Chemistry, Mar Athanasius College, Kothamangalam, Kerala, India

[c]Department of Chemistry, Union Christian college, Aluva, Kerala, India

[d]Department of Chemistry, Central University of Rajasthan, Bandar Sindri, Rajasthan, India

[e]Chemistry Division, Bhabha Atomic Research Centre, Mumbai 400 085, India

*E-mail: rajithomas28@yahoo.com

Received 20 August 2020; revised and accepted 09 February 2021

Complexes of the general formula $Cp_2Ti(IV)L$, $Cp_2Zr(IV)L$, $Cp_2Ti(IV)L^1$ and $Cp_2Zr(IV)L^1$ have been synthesized with N,N'-bis(2-pyridyl)pyridine-2,6-dicarboxamide (H_2L) and 9,10-phenanthrenequinone dioxime (H_2L^1). The complexes have been characterized by different spectral techniques and their reduction reactions have been carried out with hydrated electron as reducing radical, mechanism which has been explored pulse radiolytically. Theoretical calculations have been performed to understand the effect of chelation and electron transfer processes in complexes.

Keywords: Ti(IV)/Zr(IV) complex, Oxime complex, amide complex, hydrated electron, Pulse radiolysis

Amides and oximes are the two important precursors in the field of coordination chemistry and both react with many transition metals. The structural analyses of these complexes have been reviewed by many researchers[1, 2]. In the case of amide ligands special attention has been focused on pyridine carboxamide ligands due to their efficiency for the formation of transannular bonding. These are biologically potent ligands and their several biological significance have been reviewed[3].

Titanium complexes are active catalysts for α-olefin polymerization and for the ring-opening polymerization of cyclic esters[4, 5]. For a long time, not much has been published on the complexation of Ti and Zr halides with the oxime and amide ligands. Electron transfer and coordination chemistry overlap in many important areas of biological and structural interest because biological activities of metal complexes may be related to the redox behaviours[6]. The pulse radiolysis technique provides a means for producing low concentrations of powerful reducing and oxidizing agents on the microsecond timescale. This rapid time resolution facilitates the detection of reactive transients. Since first characterization of iminoxyl radical by Thomas in 1964, a number of studies have been reported for electron transfer behaviour of oximes[7]. There are many reports on the synthesis of transition metal complexes[8, 9]. But pulse radiolysis studies on Ti(IV) and Zr(IV) complexes of oximes and amides are virtually non-existant. In recent years, increasing effort has been devoted to the study of effect of chelation and electron transfer in complexes by quantum chemical methods, and in this respect, DFT has emerged as a useful methodology to support and/or predict experimental data[10]. Herein we report the synthesis, characterization, and redox behaviour of Ti(IV) and Zr(IV) complexes of N,N'-bis(2-pyridyl)pyridine-2,6-dicarboxamide (H_2L) and 9,10-phenanthrenequinone dioxime (H_2L^1).

Materials and Methods

All the chemicals have been purchased from Merck and Aldrich and used without further purification. All the reactions were carried out under dry conditions. Solvents were dried by standard methods[11]. IR spectra were recorded in KBr pellets on a Schimandzu spectrometer in the range 4000-400 cm^{-1}. The ^1H ($CDCl_3$, DMSO, 300 MHz) and ^{13}C ($CDCl_3$, DMSO, 75.5 MHz) NMR spectra of complexes have been obtained on a JEOL AL-300FTNMR spectrometer

using TMS as an internal standard. The melting points are recorded on Perfit melting point apparatus and are uncorrected. Nitrogen was estimated as reported in the literature method[12].

Computational calculations were performed at the DFT/B3LYP level using Gaussian suite of programs[13]. The ligands are optimized using the 631-G basis set and titanium complexes are optimized by mixed basis set (LanL2DZ for titanium and 631-G for other atoms). Larger zirconium complexes are optimized using LanL2DZ basis set.

Pulse radiolysis, kinetic and spectrophotometric measurements were made with a computer controlled instrument described previously[14]. For pulse radiolysis, Linear Accelerator Facility (PULAF) in Pune University, NCFRR, India was used to measure the kinetics and transient absorption spectra and a detailed report of the PULAF have been published[15]. This is a 7 MeV S-band linear accelerator system and having capacity of producing a range of pulse widths (10, 20, 50, 100, 200, 400 ns and 3 μs). The PULAF is coupled to the optical detection system supplied by Luzchem, Canada by which we obtain the absorption spectra for the transient species.

During the pulse radiolysis, the potassium thiocyanate dosimetry was used in which an aerated 10 mM aqueous solution of KSCN was applied and the reactive radicals formed from the radiolysis of water, the hydrated electrons (e^-_{aq}) and hydrogen radicals ($H^\bullet$) are scavenged by dissolved oxygen. The hydroxyl radical ($OH^\bullet$) oxidizes $SCN^-$and produces $(SCN)_2^{\bullet-}$.

$$SCN^- + OH^\bullet \rightarrow SCN^\bullet + OH^-$$

$$SCN^\bullet + SCN^- \rightarrow (SCN)_2^{\bullet-}$$

In most of our experimental measurements, a typical dose of 11 Gy was used. The samples for pulse radiolysis were prepared by dissolving the compound in water and this was purged using Iolar grade (Indian Oxygen Ltd.) ultra pure N_2. The distilled water was further purified in a Millipore milli-Q system. The complex is stable towards hydrolysis at least for 5 h as checked by its ground state spectra.

In the radiolysis of aqueous solutions, the reactive species formed are solvated electrons (e_{aqu}^-), $^\bullet$OH. radicals and H atoms :

$$H_2O \xrightarrow{\text{ionizing radiation}} e^-_{aq}\,(2.7), \dot{O}H\,(2.8), \dot{H}\,(0.6), H^+\,(2.7), H_2O_2\,(0.6), H_2\,(0.43)$$

The numbers in the parentheses represent the *G* values of the species, *i.e.* the number of molecules per 100 eV of absorbed energy. In the case of e^-_{aq}, the use of *tert*-butyl alcohol is generally accepted as an effective means of removing $^\bullet$OH and, to a lesser extent, the lower yield of $H^\bullet$.

$$(CH_3)_3COH + \dot{O}H \longrightarrow \dot{C}H_2C(CH_3)_2OH + H_2O, k = 6 \times 10^8$$

$$(CH_3)_3COH + H^\cdot \longrightarrow \dot{C}H_2C(CH_3)_2OH + H_2, k = 10^5$$

Synthesis of ligands

N, N'-bis(2-pyridyl)pyridine-2,6-dicarboxamide(H_2L)

To a solution of 2, 6-pyridine dicarbonyldichloride (0.408 g, 2 mmol) in dichloromethane (10 ml) at 0 °C, a solution of 2-aminopyridine (0.430 g, 4.53 mmol) in the same solvent (dichloromethane) was added. The colour of the solution changed from light green to yellow. After 15 min, triethylamine (0.5 mL) was added dropwise to the stirring mixture. Then a white precipitate began to appear and the mixture was stirred for 6 h to ensure completion of reaction. It was filtered and the precipitate was washed with saturated solution of sodium bicarbonate, water and acetone. Filtrate was dried under vacuum and ligand was obtained as white powder (60%, m.p. 215 °C).IR (KBr, cm^{-1}) ν(C=O)(1691), ν(N-H)(3354). ^{1}H NMR ($CDCl_3$, 300 MHz): δ 10.55 (s, NH), 8.63-7.31(m, ArH). ^{13}C NMR ($CDCl_3$, 75 MHz): δ 162.68(C=O), 150.88(C=N), 149.08- 123.54(C=C). Anal. Calc. for $C_{17}H_{13}N_5O_2$: C, 63.94; H, 4.10; N, 21.93. Found: C, 63.11; H, 4.03; N, 21.98%.[16]

9, 10-phenanthrenequinone dioxime (H_2L^1)

This was prepared by the literature method and the yield was 70%.[17]

Synthesis of complexes

Reaction of H_2L with dicyclopentadienyltitanium dichloride (1):

Sodium hydride (0.025 g, 1.168 mmol) was washed with hexane under dinitrogen and then added to a solution of ligand H_2L (0.186 g, 0.584 mmol) in DMF. It was allowed to stir at room temperature whereby colour changed from white to light yellowish brown solution, thereafter dicyclopentadienyl titanium dichloride (0.145 g, 0.584 mmol) in DMF was added to the above solution. A precipitate of NaCl so formed was filtered out and residual product the product was

concentrated under vacuum, washed with hexane gave a light brown product (yield :56%).

The zirconium complex (**2**) of H_2L was synthesized analogously and obtained as off white crystalline solid (77% yield).

Reaction of H_2L^1 with dicyclopentadienyltitanium dichloride (3):

To the methanolic-benzene solution (10 mL) of the sodium salt of ligand H_2L^1 (0.3573 g, 1.5 mmol) (prepared by the reaction of 9,10-phenanthrenequinone dioxime with NaOMe in methanol-benzene), the benzene solution of dicyclopentadienyltitanium dichloride (0.3734 g, 1.5 mmol) was added slowly through a dropping funnel at room temperature. The colour of the reaction mixture changed from brown to dark reddish brown. It was then stirred for 3 h to ensure completion of the reaction. The precipitated NaCl was filtered off and filtrate was dried in vaccuo, furnishing reddish brown shining compound (73%).

The zirconium complex (**4**) of H_2L^1 was synthesized analogously and obtained as yellow shining compound in 62% yield.

Results and Discussion

2, 6-Pyridine dicarbonyldichloride on treatment with a solution of 2-aminopyridine in dichloromethane produced N,N'-bis(2-pyridyl)pyridine-2,6-dicarboxamide (H_2L) in 60% yield. To a solution of H_2L in DMF, a solution of Cp_2TiCl_2 and Cp_2ZrCl_2 in DMF, respectively, were added to produce Ti (IV) and Zr (IV) amide complexes (Scheme 1). In the IR spectra, the peak at 3354 cm^{-1} was assigned to νN-H group and peak at 1691 cm^{-1}corresponded to νC=O stretching. The disappearance of amide nitrogen peak (3354 cm^{-1}) in IR spectra of both the complexes indicated deprotonation of the ligand. A subsequent formation of a new peak in the region 596.12 and 537.28 cm^{-1} assignable to νM-N stretching[18] unambiguously suggested the formation of complexes. There was no significant shifting in the carbonyl stretching indicating that no coordination from the oxygen atom of ligand to the central metal.

In ^{1}H NMR of the ligand, the signal at δ 10.55 ppm which was assigned to N-H protons and their disappearance in the complexes unfalteringly suggested the formation of metal complex. In ^{13}C NMR of H_2L, carbonyl carbon resonated at 162.68 ppm and C=N group at ~150.88 ppm. In complexes, there was no shifting of the carbonyl carbon resonances and the additional peaks in the region δ 119.64-117.81 ppm were assigned for cyclopentadienyl groups.

For the preparation of Ti and Zr derivatives, 9,10-phenanthrenequinone dioxime was first converted to its sodium salt and then reacted with biscyclopentadienylTi(IV)/ Zr(IV) dihalides in 1:1 molar ratios to form organotitanium and organozirconium complexes (Scheme 2).

Formation of Ti and Zr complexes of H_2L^1 was ascertained by the disappearance of $\nu_{(OH)}$ band which is observed at 3140-3122 cm^{-1} in H_2L^1, as well as appearance of medium intensity peak in

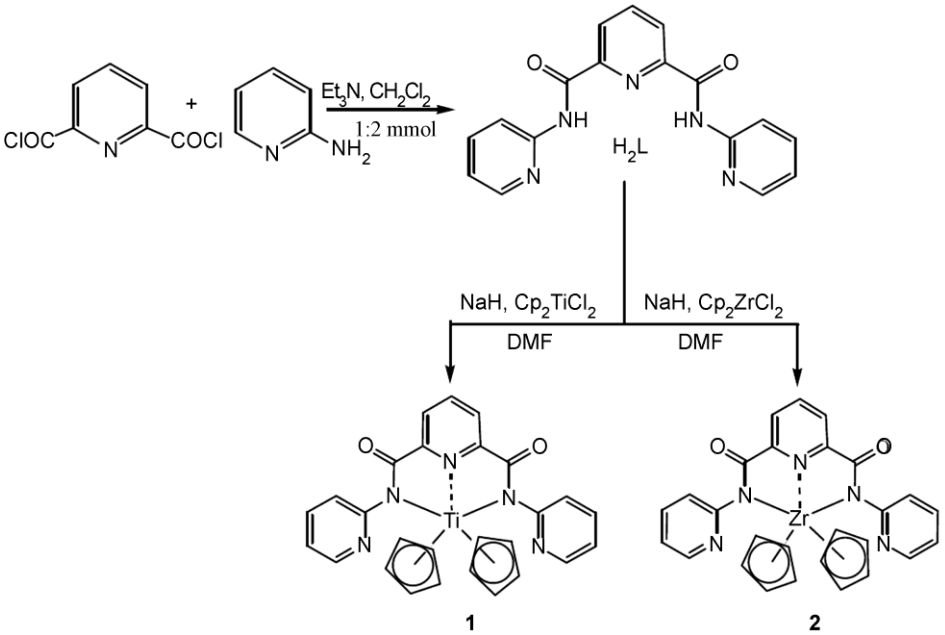

Scheme 1 — Schematic representation for the synthesis of Ti/Zr complexes of H_2L

the region 670-650 cm^{-1} assignable to $\nu_{(M-O)}$ bond[19], (spectra are uploaded as supplementary data) $\nu_{C=N}$ peak shifted from 1610-1600 cm^{-1} to 1560-1540 cm^{-1} and N-O peak shifted from 950-910 cm^{-1} to 955-940 cm^{-1} due to the electron withdrawing effect of titanium. The shifting in N-O stretching to higher frequency can be explained by the interaction between oxygen and metal; the metal drifting the electron density from nitrogen to oxygen [20] as shown below.

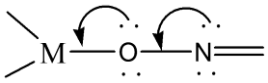

In ^{1}H NMR spectrum of oxime, the deuterium exchangeable protons of the OH group attached to C=N appeared in the range δ 12.11 ppm. In the complexes, this resonance of OH protons disappeared indicating deprotonation of =NOH group and complexation with transition metal by subsequent formation of M-O bond. cyclopentadienyl groups gave resonanced in the range δ 6.15-6.84 ppm and not much shifting being observed for phenanthrene moiety.

In the ^{13}C NMR spectra of ligand, the imine carbon of the dioxime resonated in the range δ 144.64 - 152.0 ppm whereas the aromatic carbon appeared in the range 141.2-121.6 ppm. A downfield shifting of C=N to the range 162.91-156.0 ppm upon complexation indicated the formation of complexes, the cyclopentadienyl groups resonated at δ 119.23 - 118.23 ppm. Analytical and physical data of all the complexes are shown in Table 1 and spectral data are shown in Table 2.

Computational studies

The structure, geometry and electronic properties of the complexes have been studied with the help of Gaussian 03 suite of programs. For titanium complex **1**, bond analysis gave the values of bond order of amide nitrogen with titanium in the order 0.483 (Bond length = 2.281) and that between central pyridine nitrogen and metal being 0.347. There is no coordination from side pyridine rings confirmed from their bond order 0.033. The equal bond length and bond order on both sides on the central metal concludes the symmetrical arrangement of atoms. In NBO analysis we could observe that central pyridine nitrogen interact with delocalization energy of 24.28 kcal/mol while both amide nitrogens have similar amount of delocalization energy (29.45 kcal/mol) indicating both are equally oriented

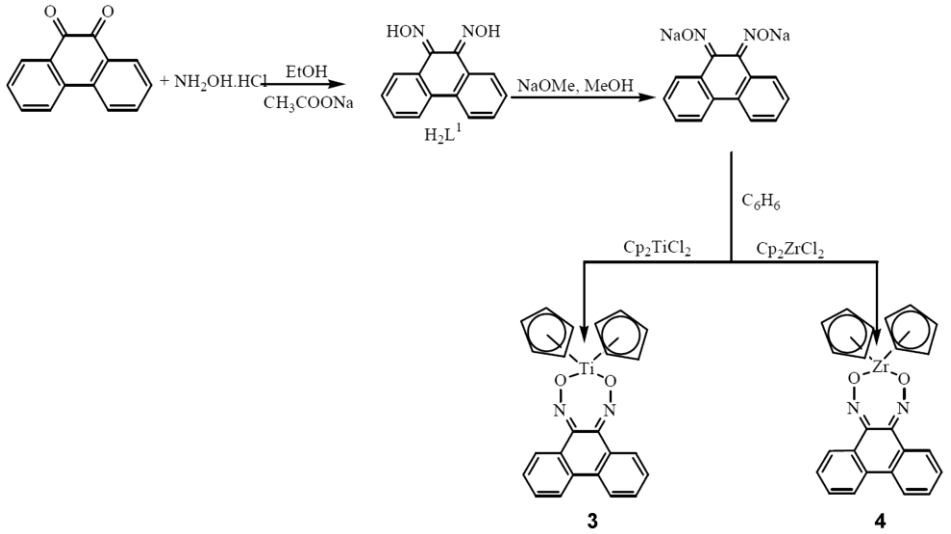

Scheme 2 — Schematic representation for the synthesis of Ti/Zr complexes of H_2L^1

Table 1 — Analytical and physical data of complexes

Compound	Colour	Mol. wt.	M. p. (°C)	Yield (%)	Elemental analysis Calc (found) (%)		
					C	H	N
1	Light brown	493.34	192	56	65.73 (65.19)	3.88 (4.01)	14.20 (14.89)
2	Off white	536.70	173	77	60.42 (60.88)	3.57 (3.27)	13.05 (13.49)
3	Dark brown	414.28	230	73	69.58 (68.38)	4.38 (4.34)	6.76 (6.55)
4	Yellow	457.64	160	62	62.99 (61.39)	3.96 (3.88)	6.12 (6.05)

so that both then interact with vacant orbitals of metal in equal amount. There is no interaction from the side pyridine ring suggesting no coordination from it.

While that of zirconium gave a bond order of 0.215 between central pyridine nitrogen and zirconium. 0.414 is obtained for bond between amide nitrogens and zirconium. Like titanium complex, in the case of zirconium complex also there is a symmetric arrangement around the central metal (NBO: Central pyridine nitrogen- 27.28 kcal/mol, amide nitrogens-32.27 kcal/mol). Optimized geometries of the complexes **1** and **2** are given in Fig. 1 (a and b).

Wiberg bond index analysis of metal-oxygen bond gave information about the bond length and bond orders. The bond length of both Ti-O in complex **3** is 1.91 Å with bond orders of magnitude 0.820 and the average distance between titanium and centers of cyclopentadienyl (Ti-Cp) are 2.45 Å each. In NBO analysis we can observe that both oxygens are equally oriented so that both interact with vacant orbitals of metal in equal amount (O1:12.15, 24.46 and 49.51, O2: 12.16, 24.46 and 49.42).

Bond analysis of the complex **4** gave O^1-Zr bond length of 2.032 Å with bond order 0.829 and O^2-Zr bond length of 2.034 with bond order 0.846. NBO analysis gave delocalization effect of lone pair of oxygen with metal. Both the oxygens are almost equally oriented so that they interact with vacant orbitals in significant manner (O^1:12.77-47.27 and O^2:11.15-51.16 kcal/mol). Optimized geometries of the complexes **3** and **4** are given in Fig. 1 (c and d).

Table 2 — Spectral characteristics of Ti(IV)/Zr(IV) complexes

Compound	IR	NMR (ppm)	
		^{1}H	^{13}C
1	$\nu_{(C=O)}$(1697), $\nu_{(Ti-N)}$(596.12)	7.81-8.73 (m, 11H, ArH), 6.19-6.73 (m, 8H, Cp-H)	162.79(C=O), 141.24-123.49(C=C), 118.29-117.43 (Cp-C)
2	$\nu_{(C=O)}$(1694), $\nu_{(Zr-N)}$(537.28)	7.27-8.91 (m, 11H, ArH), 6.16-6.35 (m, 8H, Cp-H)	162.61(C=O) 140.72-124.81(C=C), 119.47-117.22 (Cp-C)
3	$\nu_{(C=N)}$(1560), $\nu_{(NO)}$(940), $\nu_{(Ti-O)}$(650)	7.41-8.50 (m, 8H, ArH), 6.15-6.84 (m, 8H, Cp-H)	148.27(C=N), 144.18-124.37(C=C), 119.17-118.19 (Cp-C)
4	$\nu_{(C=N)}$(1540), $\nu_{(NO)}$(955) $\nu_{(Zr-O)}$(670)	7.18-8.91 (m, 8H, ArH), 6.23-6.44 (m, 8H, Cp-H)	149.94(C=N), 142.39-122.72(C=C), 119.57-117.91 (Cp-C)

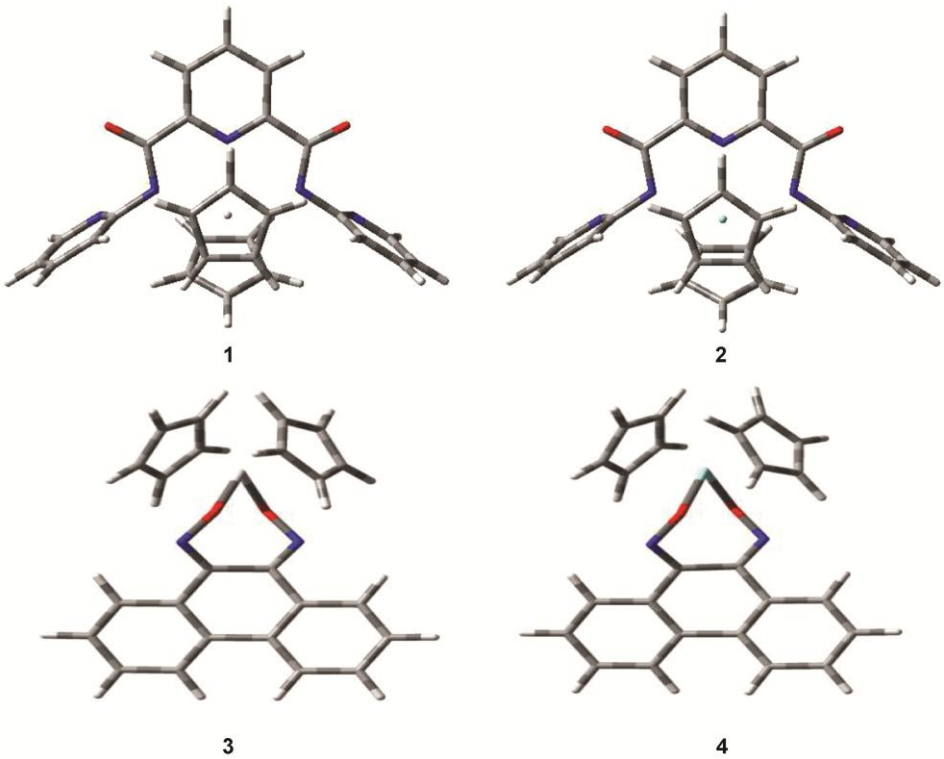

Fig. 1 — Optimized geometries of the compound **1-4**

Pulse radiolysis study

The transient species formed by the one electron reduction of oxime, amide and their Ti(IV) and Zr(IV) complexes by the hydrated electron radical as reducing radical were studied by pulse radiolysis. The rate constant of the reaction of e^-_{aq} with all ligands and complexes were measured following the decay of hydrated electron at 680 nm. In all the reactions an anion radical as transient species were formed whose characteristics are studied by optical absorption spectroscopy. In the case of amide ligand, we observed absorption peak at 350 nm due to the presence of electron localization on the pyridine ring (Fig. 2a).

The initial attack of hydrated electron is likely to occur at any of the electron deficient heteroatom oxygen or nitrogen. From the NPA charges (Fig. 2b) it is observed that most electron deficient is pyridine nitrogen and therefore the centre of attack could be C=N bond in the pyridine moiety.

There are two possibilities, one central pyridine ring and two similar side pyridine rings. Here most preferable site of attack is the side chain pyridine rings because the carbon has high positive charge due to two adjacent nitrogen atoms. This is confirmed from the NBO charges which are shown in the Fig. 2b. It will result in the formation of radical anion centered at the side pyridine ring. The electron adduct formed was likely to be highly proton affinic in nature and may result in the rapid protonation by water (Scheme 3). Similar protonation of electron adducts have previously been reported[21, 22].

The protonated species are optimized using DFT/B3LYP method using 631G basis set. The optimized structure of ligand shows the attractive electrostatic interaction between the σ framework and the π electron density in the ligand. This is mainly due to the presence of nitrogen in the ring which has an electron withdrawing effect that reduces the π electron density and thus increases π–π interactions. But this interaction disappeared in the case of protonated structure by forming a chair like conformation. The delocalization of spin density and the optimized structure of the protonated species are shown in Fig. 3.

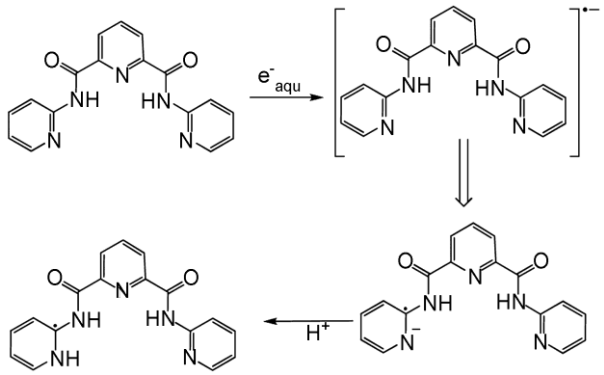

Scheme 3 — Schematic representation for the mechanism of formation of protonated species of H_2L[1]

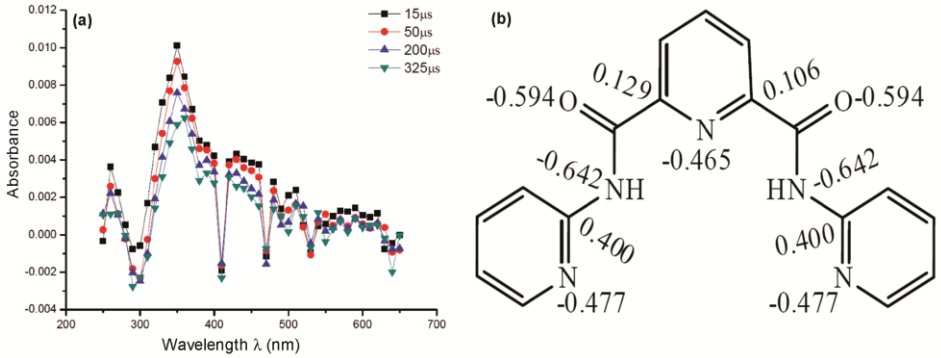

Fig. 2 — (a) Transient absorption spectra and (b) NPA charges on selected atoms of H_2L

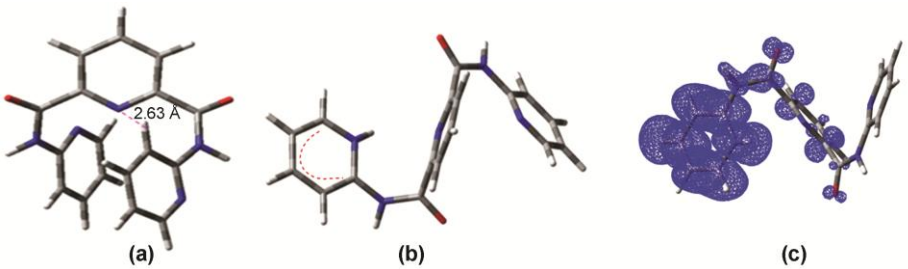

Fig. 3 — (a) Optimized structure of H_2L, (b) optimized structure of protonated species and (c) spin density distribution of the protonated species of ligand

In the case of complexes, we could observe the absorption peak which was similar to the ligand indicating the electron localization on the ligand part and with no electron transfer from ligand to metal (Scheme 4) as shown in transient absorption spectra in Fig. 4.

The anion radicals were optimized using DFT/B3LYP method using mixed basis set for Ti-complex and LanL2DZ for Zr-complex. The rate constants calculated for the amide ligand, Ti- and Zr-complexes are 1.22×10^5, 2.08×10^5, 2.74×10^2 dm^3 mol^{-1} s^{-1}, respectively.

Optical absorption spectrum of the 9, 10-phenanthrenequinone showed two major peaks; a peak at 282 nm and a high intensity peak at 400 nm (Fig. 5a). The initial attack of e^-_{aq} is likely to occur at electron deficient C=N which is confirmed from the NBO analysis as shown in Fig. 5b.

$$[Cp_2TiL] + e^-_{aq} \longrightarrow [Cp_2Ti(L)^{\bullet-}]$$

$$[Cp_2ZrL] + e^-_{aq} \longrightarrow [Cp_2Zr(L)^{\bullet-}]$$

Scheme 4 — Schematic representation for the reaction of hydrated electron on Ti/Zr complexes of H_2L

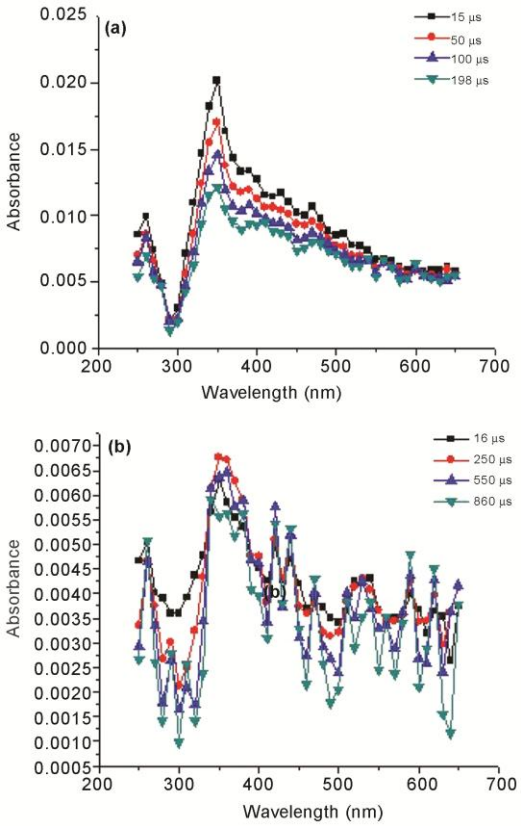

Fig. 4 — Transient absorption spectra for (a) Cp_2TiL and (b) Cp_2ZrL

A radical anion is formed as transient species by the initial attack in which the electron is mainly concentrated on the C=N bond which undergoes protonation forming the final product as shown in Scheme 5. Optimized structures of the intermediates with energy values are shown in Fig. 6.

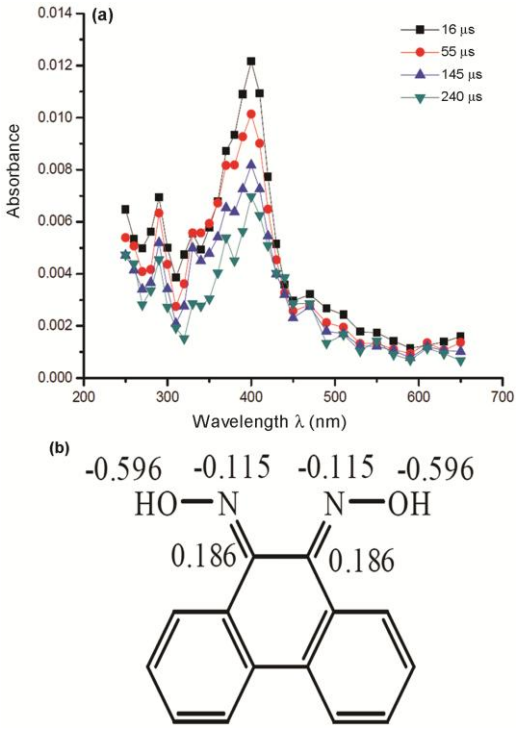

Fig. 5 — (a) Transient absorption spectra and (b) NPA charges on corresponding atom of H_2L[1]

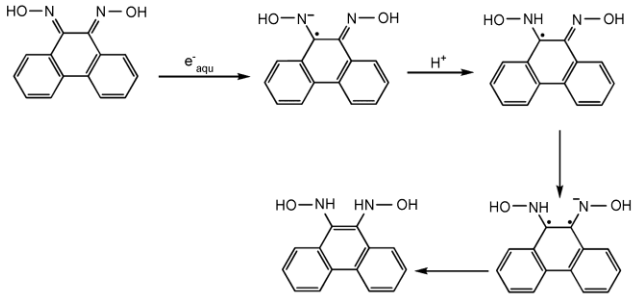

Scheme 5 — Schematic representation for the mechanism of formation of protonated species of H_2L[1]

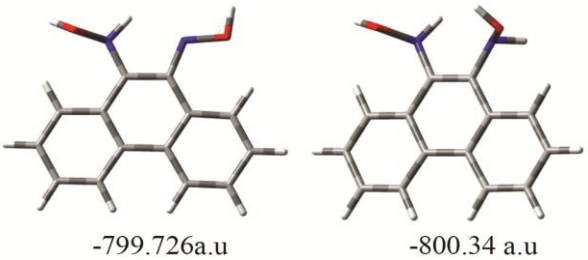

Fig. 6 — Optimized structures of the intermediates

Table 3 — Energy values for the radical anions from ligands and complexes

Species	Energy (kcal/mol)	Species	Energy (kcal/mol)	Species	Energy (kcal/mol)
$[H_2L^1]^{\bullet-}$	-799.1546	$[Cp_2TiL^1]^{\bullet-}$	-2034.5359	$[Cp_2ZrL^1]^{\bullet-}$	-1231.8313
$[H_2L]^{\bullet-}$	-1075.8248	$[Cp_2TiL]^{\bullet-}$	-2314.8779	$[Cp_2ZrL]^{\bullet-}$	-1215.2540

$$[Cp_2Ti(IV)L^1] + e^-_{aq} \longrightarrow [Cp_2Ti(III)(L^1)]$$

$$[Cp_2Zr(IV)L^1] + e^-_{aq} \longrightarrow [Cp_2Zr(III)(L^1)]$$

Scheme 6 — Schematic representation for the reaction of hydrated electron on Ti/Zr complexes of H_2L^1

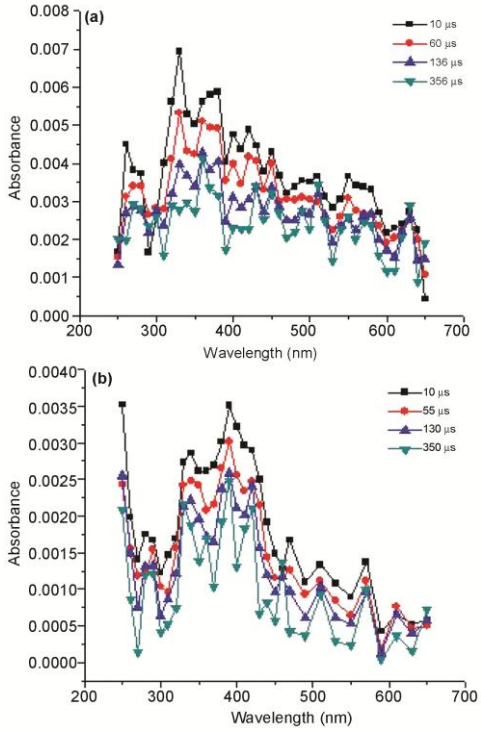

Fig. 7 — Transient absorption spectra for (a) Cp_2TiL^1 and (b) Cp_2ZrL^1

In the case of titanium complex of the oxime ligand, a shoulder in the range 270-280 nm appeared and there is no peak at 282 nm which is observed in the ligand indicating ligand to metal charge transfer resulting in Ti(III) species (Scheme 6). From the spectra we can observe various LMCT with low intensity. After hitting the electron in C=N bond the charge is transferred through the N-O bond to the metal resulting in the reduction of the metal and in the case of zirconium complex also in addition to peak at 400 nm, there are additional peaks indicating the electron is not localized on the ligand part, but it transferred to the metal resulting in the reduction. The absorption spectrums of both the complexes are shown in the Fig. 7. The rate constants calculated for the oxime ligand, Ti- and Zr-complex are 1.61×10^6, 5.26×10^5, 8.78×10^2 dm^3 mol^{-1} s^{-1}, respectively. The energy values of all the ligands, complexes and their corresponding radical anions with respect to appropriate basis set are tabulated in Table 3.

Conclusions

In the case of amide complexes the electron is localized on the ligand part i.e. no electron transfer is taking place from ligand to metal but in the case of oxime complexes the absorption peaks obtained are different from that of ligand indicating metal have a significant role in the electron transfer processes. The rate constant is highest for oxime ligand indicating fastest reaction with hydrated electron. In both type of complexes Zr-complexes have the lowest rate constant.

Supplementary Data

Supplementary Data associated with this article are available in the electronic form at http://nopr.niscair.res.in/jinfo/ijca/IJCA_60A(03)361-369_SupplData.pdf.

Acknowledgement

Financial support from DAE/BRNS is gratefully acknowledged.

References

1 Chakravorty A, *Coord Chem*, 13 (1974) 1.
2 Serin S, *Trans Met Chem*, 26 (2001) 300.
3 Cheng C C, Huang X, Shipps G W, Wang Y, Wyss D F, Soucy K A, Jiang C, Agrawal S, Ferrari E, He Z & Huang H C, *Med Chem Lett*, 1 (2010) 466.
4 Takeuchi D & Aida T, *Macromolecules*, 33 (2000) 4607.
5 Oakes D C H, Gibson V C, White A J P & Williams D J, *Inorg Chem*, 45 (2006) 3476.
6 Brown D G, *Prog Inorg Chem*, 18 (1973) 17.
7 Thomas J R, *J Am Chem Soc*, 86 (1964) 1446.
8 Dilworth J R & Parrott S J, *Chem Soc Rev*, 27 (1998) 43.
9 Leonard J P, Novotnik D P & Neirinck R D, *J Nucl Med*, 27 (1986) 1819.
10 Bagno A, Casella G & Saieili G, *J Chem Theory Comput*, 2 (2006) 37.
11 Armarego W L F & Perrin D D, *Purification of Laboratory Chemicals, 4th Edn.* (Oxford, Butterworth) 1997.
12 Vogel A I, *Textbook of Quantitative Chemical Analysis 4th Edn*, (Longman, London) 1989.
13 Gaussian 03 Revisions D O I, Frisch M J, Trucks G W, Schlegel H B, Scuseria G E, Robb M A, Cheeseman J R,

Montgomery J A, Vreven T, Kudin K N, Burant, J C, Millam J M, Iyengar S S, Tomasi J, Barone V, Mennucci B, Cossi M, Scalmani G, Rega N, Petersson G A, Nakatsuji H, Hada M, Ehara M, Toyota K, Fukud R, Hasegawa J, Ishida M, Nakajima T, Honda Y, Kitao O, NakaiH, Klene M, Li X, Knox J E, Hratchian H P, Cross J B, Bakken V, Adamo C, Jaramillo J, Gompert R, Stratmann R E, Yazyev O, Austin A J, Cammi R, Pomelli C, Ochterski J W, Ayala P Y, Morokuma K, Voth A Salvador P, Dannenberg J J, Zakrzewski V G, Dapprich S, Daniels A D, Strain M C, Farkas O, Malick D K, Rabuck A D, Raghavachari K, Foresman J B, Ortiz J V, Cui Q, Baboul A G, Clifford S, Cioslowski J, Stefanov B B, Liu G, Liashenko A, Piskorz P, Komaromi I, Martin R L, Fox D J, Keith T, Al-Laham M A, Peng C Y, Nanayakkara A, Challacombe M, Gill P M W , Johnson B, Chen W, Wong M, Gonzalez C & Pople J A, *Gaussian 98, revision A 5*, Gaussian, Inc. Pittsburgh (1998).

14 Patterson L K & LilieJ J, *Int J Radiat Phys Chem*, 6 (1974) 129.

15 Yadav P, Kulkarni M S , Shirdhonkar M B & Rao B S M, *Curr Sci*, 92 (2007) 599.

16 Raji T & Pushpa P, *Asian J Chem*, 32 (2020) 995.

17 Thomas R, Joseph N P, Pardasani R T, Pardasani P & Mukherjee T, *Helv Chim Acta*, 96 (2013) 1740.

18 Bradley D & Gitlitz M, *Nature*, 218 (1968) 353.

19 Davidson M G, Johnson A L, Jones M D & Mahon M F, *Polyhedron*, 26 (2007) 975.

20 Buyuktas B S & Aktas O, *Trans Met Chem*, 31 (2006) 56.

21 Sonntag C, *The Chemical Basis of Radiation Biology*, (Taylor and Francis, London) 1987.

22 Steenken S, *Chem Rev*, 89 (1989) 503.